

Figure 1 Schematic showing the geometry used in these experiments. (a) Top view. (b) Side view, looking down the z axis. The angle μ is fixed for the particular reciprocal section of interest and ω is rotated through 2π while the image plate is translated by its full width behind the slit.

vertical slit. The detection slits consist of two Pb plates, 200 mm wide, 250 mm high, 3 mm thick, and spaced 0.5 mm apart. The angles μ and ξ , which define how the sample rotation axis and detection slits are oriented with respect to the incident beam, are kept constant during the crystal rotation. Here, we set μ and ξ , that is, we used Weissenberg flat-cone geometry, which has been described in detail by Buerger (1942) and Osborn & Welberry (1990). A particular layer normal to the crystal rotation axis is selected by the choice of μ . If a Cartesian coordinate system is attached to the sample such that the crystal rotation axis is z and the x axis is horizontal and the y axis vertical when $\omega = 0$, then the components of the scattered wavevector along the three coordinate axes can be related to the angles ω , μ and η by (Osborn & Welberry, 1990)

$$\lambda k_x = +\cos(\eta - \omega) - \cos \mu \cos \omega, \quad (1)$$

$$\lambda k_y = -\sin(\eta - \omega) - \cos \mu \sin \omega, \quad (2)$$

$$\lambda k_z = +\sin \mu, \quad (3)$$

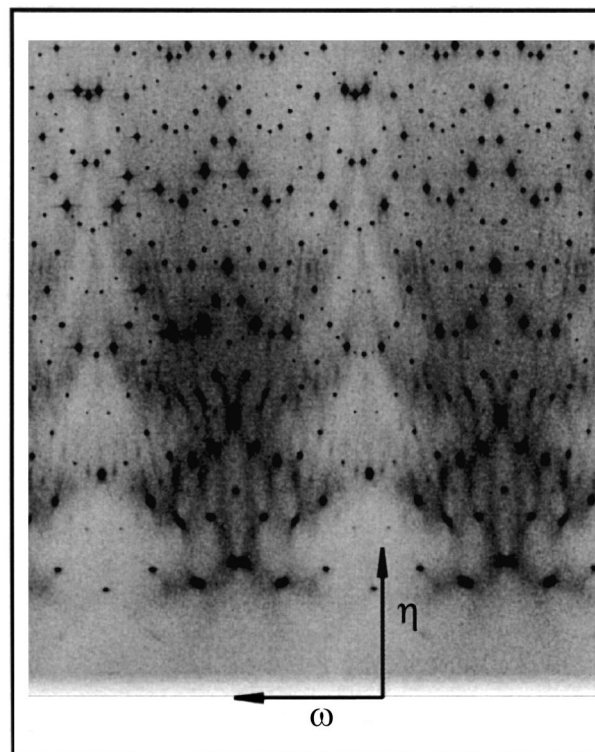


Figure 2 Raw data from the storage phosphor image plate taken at an angle $\mu = 0.059^\circ$, corresponding to the reciprocal layer $a^* = 0.05$. The ‘undistorted’ diffraction image from this plate is shown in Fig. 3.

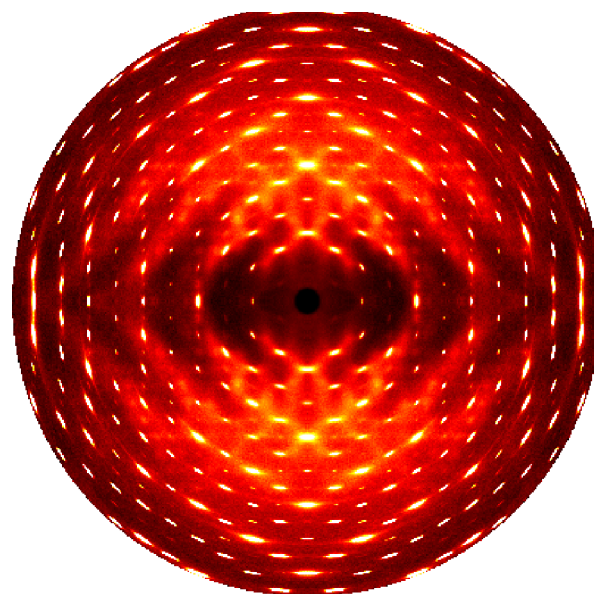


Figure 3 Undistorted diffuse scattering image produced from the data displayed in Fig. 2. Here \mathbf{b}^* is horizontal and \mathbf{c}^* is vertical. This figure contains data to a scattering angle of 26° , which at photon energies of 45 keV are beyond the accessible wavevector range of a Cu anode source.

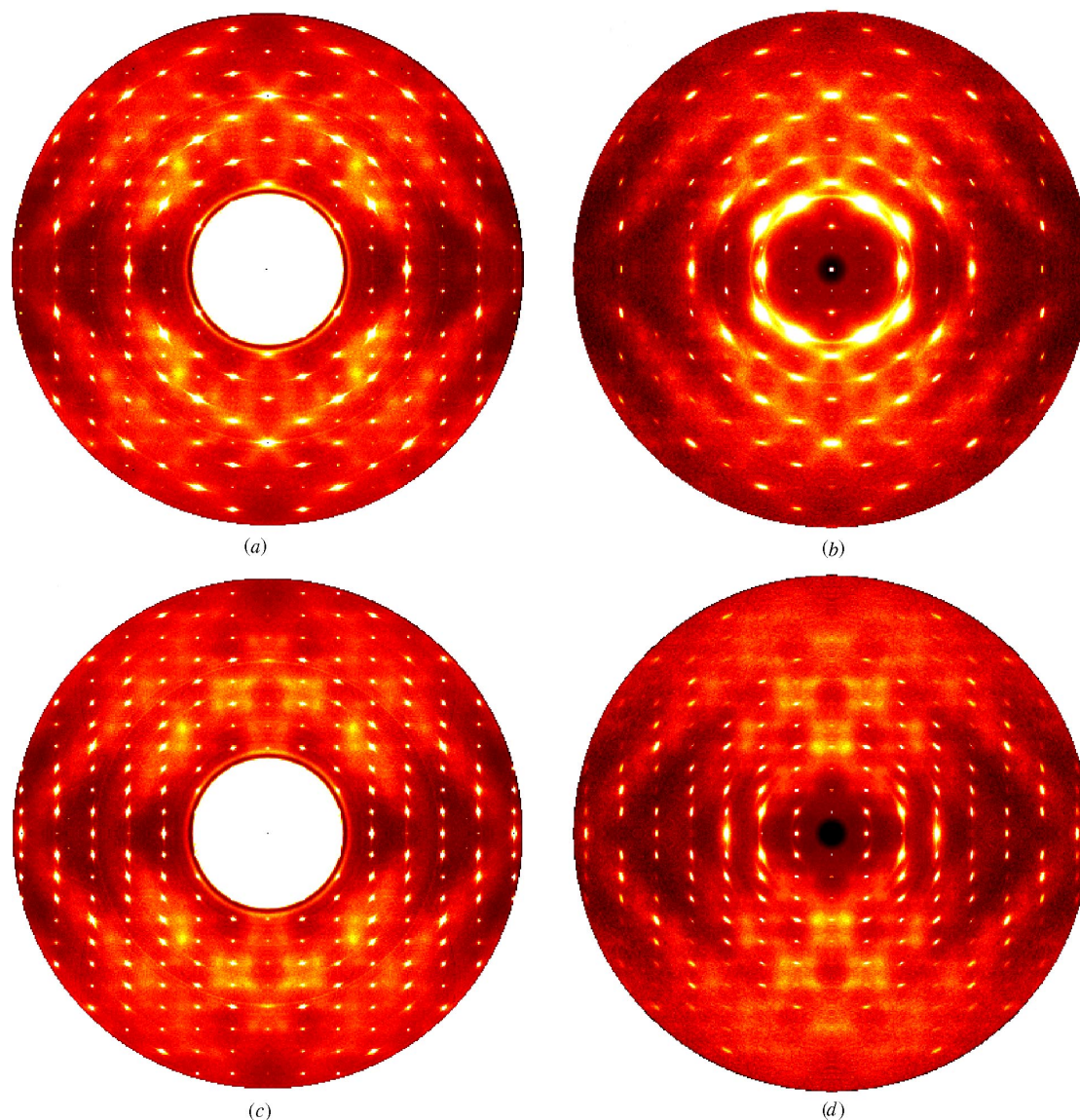


Figure 4 Comparison of data collected using a conventional sealed-tube source (Welberry & Mayo, 1998), images (a) and (c), with data recorded at high energies, images (b) and (d). Images (a) and (b) are from the (0kl) layer, while (c) and (d) are from the (1kl) layer. (b) and (d) were recorded with a sample to image-plate distance of 683 mm.

where λ is the X-ray wavelength and the wavevector magnitude is

$$k = 2 \sin(\theta)/\lambda. \quad (4)$$

The scattering angle 2θ can be obtained from

$$\cos 2\theta = \cos \eta \cos \mu. \quad (5)$$

The radial δk_ρ and tangential δk_ϕ resolution in the xy reciprocal plane are related to the angles η and μ and the divergence of the instrument along η , $\delta\eta \simeq d/l$, where d is the diameter of the crystal and l is the sample to detector distance:

$$\delta k_\rho = \delta\eta \sin \eta \cos \mu / \{\lambda[(\cos \eta - \cos \mu)^2 + \sin^2 \eta]^{1/2}\} \quad (6)$$

and

$$\delta k_\phi = \delta\eta(1 - \cos \eta \cos \mu) / \{\lambda[(\cos \eta - \cos \mu)^2 + \sin^2 \eta]^{1/2}\}. \quad (7)$$

For small angles μ , these relations can be simplified to

$$\delta k_\rho = \delta\eta \cos(\eta/2)/\lambda \quad (8)$$

and

$$\delta k_\phi = \delta\eta \sin(\eta/2)/\lambda. \quad (9)$$

Note that

$$(\delta k_\rho^2 + \delta k_\phi^2)^{1/2} = \delta\eta/\lambda. \quad (10)$$